Smart Structures and Systems, *Vol. 18, No. 4 (2016) 643-662*
DOI: http://dx.doi.org/10.12989/sss.2016.18.4.643

Active monitoring of pipeline tapered thread connection based on time reversal using piezoceramic transducers

Xiaobin Hong[1,2], Gangbing Song[*2,3], Jiaobiao Ruan[2], Zhimin Zhang[2,4], Sidong Wu[1] and Guixiong Liu[1]

[1]*School of Mechanical and Automotive Engineering, South China University of Technology, Guangzhou, Guangdong, 510641, People's Republic of China*
[2]*Smart Material and Structure Laboratory, Department of Mechanical Engineering, University of Houston, Houston, TX 77004, USA*
[3]*School of Civil Engineering, Dalian University of Technology, Dalian, Liaoning, 116023, People's Republic of China*
[4]*Institute of Applied Physics, University of Electronic Science and Technology of China, Chengdu, Sichuan, 610054, People's Republic of China*

(Received May 15, 2014, Revised September 22, 2014, Accepted October 27, 2014)

Abstract. The monitoring of structural integrity of pipeline tapered thread connections is of great significance in terms of safe operation in the industry. In order to detect effectively the loosening degree of tapered thread connection, an active sensing method using piezoceramic transducers was developed based on time reversal technique in this paper. As the piezoeramic transducers can be either as actuators or sensors to generate or detect stress waves, the energy transmission for tapered thread connection was analyzed. Subsequently, the detection principle for tapered thread connection based on time reversal was introduced. Finally, the inherent relationship between the contact area and tightness degree of tapered thread connection for the pipe structural model was investigated. Seven different contact area scenarios were tested. Each scenario was created by loosening connectors ranging from 3 turns to 4.5 turns in the right tapered threads when the contact area in the left tapered threads were 4.5 turns. The experiments were separately conducted with a highly noisy environment and various excitation signal amplitudes. The results show the focused peaks based on time reversal have the monotonously rising trend with the increase of the contact areas of tapered threads within an acceptable monitoring resolution for metal pipes. Compared with the energy method, the proposed time reversal based method to monitor tapered threads loosening demonstrates to be more robust in rejecting noise in Structural Health Monitoring (SHM) applications.

Keywords: Structural Health Monitoring (SHM); pipeline tapered thread connections; piezoceramic transducers

1. Introduction

Tapered thread connections are widely used in a variety of pipeline networks, such as those found in city water pipelines, food industry, pharmaceutical factory, channel for oiling and steam

*Corresponding author, Professor, E-mail: GSong@Central.UH.EDU

Copyright © 2016 Techno-Press, Ltd.
http://www.techno-press.org/?journal=sss&subpage=8 ISSN: 1738-1584 (Print), 1738-1991 (Online)

pipeline, since they processes good centering ability, easy assembly and disassembly, bearing capacity for larger axial force, long lifetime, good interchangeability and reusability. Failures occurring in tapered thread connections are the main consequences leading to pipeline accidents (Andrieux and Leger 1993). The loosened tapered thread connection is one of the key failure contributors. Application of Structural Health Monitoring (SHM) in threaded connections will have a greatly positive effect on the safety and reliability of pipeline structures (Bouchoucha *et al*. 2012). As one of promising active SHM techniques for engineering structures, the piezoelectric Lead Zirconate Titanate (PZT)-based approach has been widely recognized. PZTs have many advantages, such as the availability of different shapes, broadband response frequency, low price and the ability of being employed as actuators or sensors (Shi and Zhang 2008). A new technology called smart aggregate that uses embedded piezoceramic based transducers has been used to monitor cracks in concrete structures (Song *et al.* 2006, 2007, 2008, Laskar *et al.* 2009, Liao *et al.* 2011). Recent studies show that one potential SHM application using piezoelectric sensor networks is the monitoring for pipelines or pipe-like hollow structure. For example, Tua *et al.* (2005) studied the detection of cracks in cylindrical pipes and plates using piezo-actuated Lamb waves. Wang *et al.* (2010) presented the experimental investigation of reflection in guided wave-based inspection for the characterization of pipeline defects. Furthermore, the PZTs were applied in the welded areas of pipelines. For example, Rezaei *et al.* (2010) discussed health monitoring of pipeline girth weld using empirical mode decomposition with PZTs. And Lu *et al.* (2011) investigated the propagation of guided waves (GWs) using the finite element method (FEM) and experimental analysis with the purpose of evaluating welding damage in tubular steel structures. For objects inside pipeline structures, for example, Ma *et al.* (2007) investigated the feasibility study of sludge and blockage detection inside pipes using guided torsional waves. Moreover, they presented the measurement method of the properties of fluids inside pipes using guided longitudinal waves. For communication on pipeline structures, Mijarez *et al*. (2009) presented an automatic guided wave pulse position modulation system using tubes as a communication channel for detecting flooding in the hollow sub-sea structures of offshore oil rigs. Kokossalakis (2006) proposed to use the pipeline as an acoustic waveguide produced by PZTs for the transmission of appropriately modulated acoustic waves that encapsulate the digital signal, since radio frequency transmission is not feasible underground. For thread failure of pipeline structures, He *et al*. (2003) presented a detection method for oil tube threads, which combines optical techniques and image processing techniques to measure the physical dimension of tube thread to allow further analysis. Chen *et al*. (2010) presented an analytical method that can compute the load distribution on the thread teeth in cylindrical pipe threaded connections. Wang *et al.* (2013) presented a piezoceramic based active sensing method aiming at monitoring bolt connection status and detecting bolt loosening. From above, it is known that PZTs had been effectively applied in the different aspects of pipelines structure integrity detection. However, the issue about the monitoring for loosening tapered threads, which are mainly used for pipe connection and all kinds of accessories connected with pipeline, is still not taken into account and neglected by most authors. It will be a new attempt to detect quantitatively the loosening of pipeline threads using PZTs.

In recent years, the time reversal technique is receiving increasing attention. And particularly it has also been introduced to the field of SHM in connection with the two operation modes using PZTs, including passive sensing mode and active sensing mode. For passive sensing mode, Vigoureux and Guyader (2012) used time reversal method to localize the origin of the vibration detected on the surface of a structure. Ciampa and Meo (2011, 2012) presented an imaging method

based on time reversal to detect in real-time the impact source location in reverberant complex composite structures using only one passive sensor. This technique was applied to a number of waveforms stored in a database containing the impulse response (Green's function) of the structure. A combination of time reversed acoustics and nonlinear elastic wave spectroscopy techniques was introduced to localize surface breaking defects in a non-destructive manner by Damme *et al.* (2012). Simultaneously, the active sensing mode has become a hot spot method for large structures. For example, Parka *et al.* (2007) proposed time reversal active sensing for health monitoring of a composite plate. And a wavelet-based signal processing technique was developed to enhance the time reversibility of Lamb wave in thin composite plates. Time reversal active sensing using Lamb waves was investigated for health monitoring of a metallic structure by Gangadharan *et al.* (2009). Watkins *et al*. (2012) developed a time reversal method and presented diagnostics of damage in a composite plate based on Lamb waves using time reversal of signals. Additionally, Jun and Lee (2012) proposed a baseline-free time reversal process (TRP)-based SHM technique, which was characterized by two key features: the hybrid TRP (HTRP) and the diagnostic digital imaging method.

In the previous studies by Hong *et al.* (2013), the tapered thread loosening cases in a pipeline with nine connectors at different locations were identified by a pattern recognition method. However the degree of the loosening have not detected yet. In this study, the active monitoring method for tapered threads connection loosening based on time reversal using piezoelectric transducers is proposed to detect the loosening degree and the performance of the approach is validated with a pipeline structure model with tapered thread connection. Two piezoceramic patches will be respectively bonded on the two different pipe parts that are connected by a pipe connector through tapered threads. In the proposed active sensing approach, one piezoceramic patch is used as an actuator to generate an elastic stress wave, and the other one is used to detect the wave that propagates through the tapered thread connection. The received energy depends on the contact area which can be adjusted by the fastening force. The focused peak method based on time reversal for tapered thread connection loosening was proposed. By analyzing the received signals based on time reversal, the status of tapered threads loosening can be detected. To study the effectiveness of the proposed method, the pipe structure model tests with tapered thread connection were performed in the Smart Materials and Structures Laboratory (SMSL) at the University of Houston (UH). The results were analyzed and compared between the proposed method and energy method.

2. Detection principle for tapered thread connection loosening based on time reversal

As shown in Fig. 1, pipeline threads manifest mostly in the form of special tapered seal with threaded graves. By tightening the threads, a well fitted tapered thread with enough end face margin could shift axially, and generate preload force on the junction surface. In order to maintain sealing capacity, a ring-like contact region with continuous uninterrupted pressure must form on the junction surface, in which interference fit is achieved. Furthermore, with enhancement of the machining quality and axial force of the junction surface, the contact region could be larger with more compression. In classical Hertzian contact theory (Yang and Chang 2006), the true contact area A_t has a relationship with normal pressure p as shown

$$A_t \propto \sqrt{p} \tag{1}$$

In addition to that, an enlarged contact area could also reduce the chances of pipe leakage and improves better seal performance.

2.1 Active monitoring principle using piezoelectric transducers based on energy method

Two pieces of PZTs are respectively bonded on the different sides of the interface as an actuator and a sensor, as shown in Fig. 2. PZT1, as an actuator, generates a stress wave that propagates across the tapered thread contact interface, and then the signal is captured by PZT2, which is a sensor. Propagating waves are the means of power transmission between the PZTs. As illustrated in Fig. 2, some of the incident energies of the waves generated by PZT1 are transmitted to PZT2 as effluent energy, and the other energies are dissipated at the thread connect ion interface. With the increase of contact area, more energy is transmitted to the sensor PZT2 (Antoyuk *et al*. 2010). The transmitted energy E is proportional to the true contact area (Wang *et al*. 2013, Yang and Chang 2006) in a certain range as shown

$$E \propto A_t \tag{2}$$

By analyzing the change of the energy transmitted to the sensor PZT2, a relationship can be established between the amount of contact area and the received energy. For the received digital signal, the signal energy can be expressed as a second norm of the sensor signal in the discrete time domain $[t_s, t_f]$ as follows

$$E = \frac{1}{f_s} \sum_{t=t_s}^{t_f} y^2(t) \tag{3}$$

where $y(t)$ and f_s denote the received discrete signal and its sampling frequency, respectively. Under different contact areas, the transmitted energy through an interface of the connective tapered threads will be different. However, the energy method may be affected by the noise as

$$y(t) = s(t) + n(t) \tag{4}$$

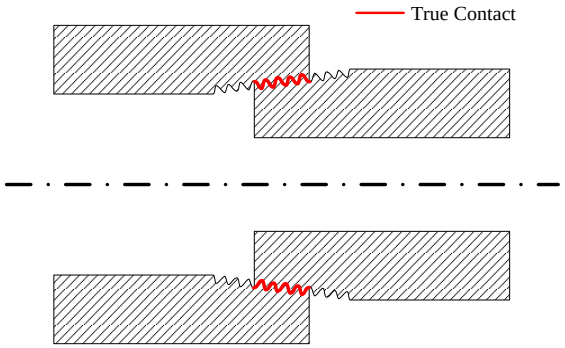

Fig. 1 Sectional interface for tapered threads

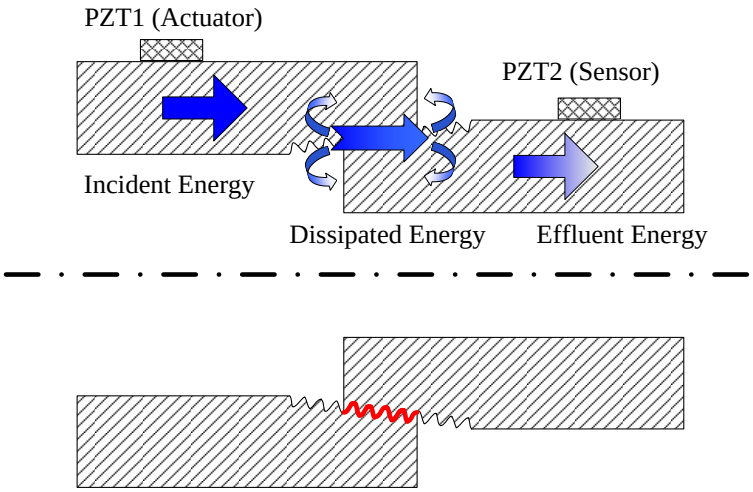

Fig. 2 Energy transmission at the microcontact interface

where $s(t)$ is the real signal, and $n(t)$ is the noise. By combining the Eqs. (3) and (4), one can see that the energy is related to the noise, and that the different noise leads to the different measure results. In order to solve the problem, the detection principle for tapered thread connection loosening based on time reversal technique was proposed in the paper.

2.2 Active monitoring principle for tapered threads connection using PZTs based on time reversal

The theoretical analysis of focused peak based on time reversal process is discussed in Fig. 3. Two short steel pipes are fastened by a pipe fitting with tapered threads, and PZT patches are mounted on the two steel pipes surfaces as an actuator and a sensor, respectively. A pulse input $x(t)$ is generated by PZT1 and propagates through the pipe whose impulse response function is represented by $h(t)$. The received signal $y(t)$ from PZT2 can be written as

$$y(t) = x(t) \otimes h(t) \tag{5}$$

where $\otimes$ denotes the convolution operation. Then the time reversal process is implemented by means of the received signal. The time reversal signal of $y(t)$ in the time domain can be written as

$$y(-t) = x(-t) \otimes h(-t) \tag{6}$$

where $x(-t)$ is the reversal signal of $x(t)$ in time domain. Subsequently, the time reversed signal is sent from PZT2 back to PZT1. The focused signal received by PZT1, namely $y^{TR}(t)$, can be written as

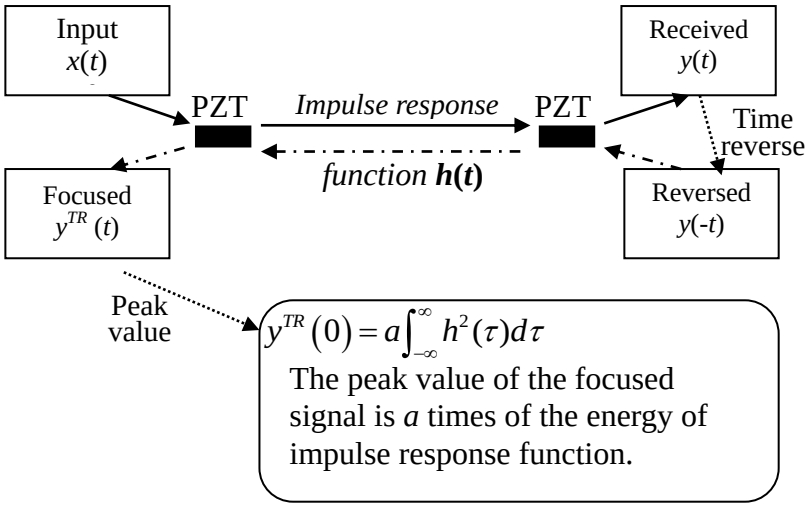

Fig. 3 Theoretical process of focused peak based on the time reversal process

$$y^{TR}(t) = y(-t) \otimes h(t) = x(-t) \otimes [h(-t) \otimes h(t)] \tag{7}$$

where $h(-t)$ means the same transmission medium as described by $h(t)$ in Eq. (5). Using the properties of convolution and correlation operations, Eq. (7) can be rewritten as

$$y^{TR}(t) = x(-t) \otimes [h(t) \square h(t)] \tag{8}$$

where $\square$ denotes the correlation operation. Pulse inputs adopted for damage detection are usually symmetric with respect to time, and thus can be expressed as $x(-t) = x(t)$. For time reversal symmetric pulse input, Eq. (8) can be simplified to a convolution of input signal $x(t)$ and the time reversal operator $h(t) \square h(t)$. The time reversal operator is usually represented by $g^{TR}(t)$ and can be expressed as

$$g^{TR}(t) = \int_{-\infty}^{\infty} h(\tau) h(\tau + t) d\tau \tag{9}$$

Clearly, Eq. (9) indicates that the time reversal operator is an even function, which therefore makes the focused signal time reversal symmetric in the time domain due to the other time reversal symmetric input $x(t)$. When $t = 0$, Eq. (9) becomes

$$g^{TR}(0) = \int_{-\infty}^{\infty} h^2(\tau) d\tau \tag{10}$$

From the Eq. (10), it is clear that $g^{TR}(0)$ is the maximum value of time reversal operator, and is also equal to the energy of impulse response function representing structural condition. Since

$g^{TR}(t)$ is the auto-correlation function of impulse response $h(t)$, which is uncorrelated to noise, the peak amplitude $g^{TR}(0)$ will not be affected by noise. Therefore, time reversal method has a robust anti-noise ability and it will be reliable in a low SNR environment. Moreover, considering that the pulse input can be expressed as $x(t)=a\delta(t)$, where $\delta(t)$ denotes unit pulse, Eq. (8) can be expressed as

$$y^{TR}(t)=ag^{TR}(t)=a\int_{-\infty}^{\infty}h(\tau)h(\tau+t)d\tau \tag{11}$$

where a is the amplitude of the input signal. From Eq. (11), it can be easily found that the peak value of the focused signal is a times of the energy of impulse response function and the peak amplitude is proportional to input amplitude with the same $h(t)$.

As the time reversal focused peak amplitude measures the impulse response energy with anti-noise ablity, and the impulse response energy is determined by the contact area, the peak value can be used to indicate the tapered thread connection tightness. As Fig. 3 shows, it is the theoretic process to obtain focused signal peak amplitude.

3. Experimental setup

Fig. 4 is the picture of experimental platform for active structural monitoring on tapered thread connection in Smart Materials and Structures Laboratory at University of Houston. The picture of pipe structure model with the tapered threads connector is shown in Fig. 5, which consists of one pipe connector and two short pipes. The two short pipes were assembled together by the pipe connector with tapered threads, where the inclined angle is 30 degrees. PZT1 and PZT2 were mounted on the outside surface of the pipes. Fig. 6 is the zoomed in photo of PZT patch transducer. Each PZT patch were bonded onto the pipe surface with nonconductive epoxy and the top of each patch was covered with nonconductive epoxy to protect from damage. The pipe connector can be fixed on a vice clamp and different levels of loosening can be adjusted by the free pipes. Upon excitation, the actuator generates elastic waves that propagate through the tapered threaded connector, interrogating the loosening degree of connector structures, and thus providing information on the operating conditions of the pipe joint. In this experiment, different loosening degrees of the tapered thread pipe connector should be identified.

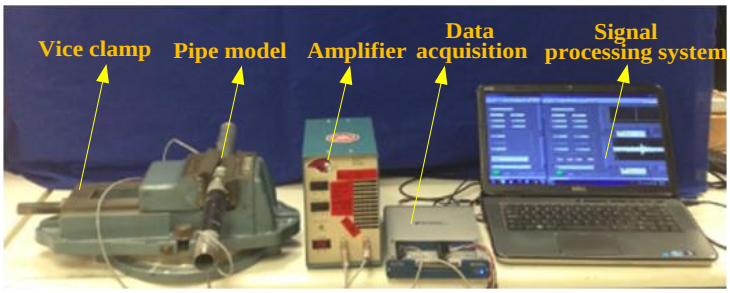

Fig. 4 Experimental setup

Fig. 5 Pipe structure model with left and right tapered threads

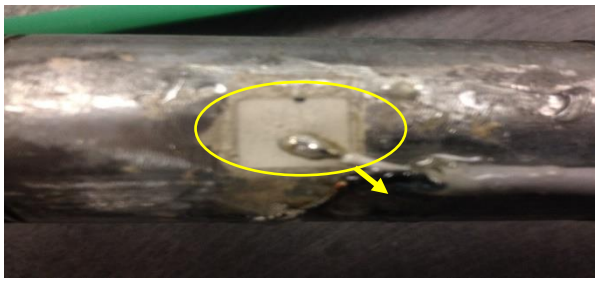

Fig. 6 Zoom in picture of the PZT transducer

4. Experimental results and analysis

4.1 The relationship between stress wave transmission and contact area of tapered thread connection

The Gaussian pulse $E(t)$ is a typical ultra-wideband (UWB) signal with a short duration in the time domain, whose expression is

$$E(t) = \exp(-\frac{4\pi(t-t_0)}{\tau^2}) \tag{12}$$

where τ is a constant determining Gaussian pulse width, and the peak appears at $t = t_0$. The Fourier transform of Eq. (10) is

$$E(f) = \frac{\tau}{2}\exp(-j2\pi ft_0 - \frac{\pi f^2\tau^2}{4}) \tag{13}$$

This paper adopted the second derivative of Gaussian function to generate a pulse waveform. The pulse waveform with a central frequency of 10 KHz and a bandwith of 1.5 is shown in Fig. 7.

There is a relationship between the applied torque and the tightness of tapered threads. However, in various meshing processes of tapered threads, it was found that a same torque could correspond to different contact areas. Therefore, the torque does not have the uniqueness to monitor the tightness of tapered thread connection, and is unacceptable as monitoring variable. By contrast, the certain correspondence between the tightness and the contact area provides feasible

evidence to study the relationship between stress wave and tightness over different contact areas (Shahani and Sharifi 2009). To find this relationship correctly, the contact area of left tapered threads of the pipe structure model was fixed, while that of right tapered threads can be adjusted in monotonically increasing intervals.

As for the chosen pipeline, it was known that the tapered threads would become highly tightened when its contact region is greater than 4 turns; therefore the contact area of the left tapered thread was fixed at 4.5th turn. In practical applications, since alarming status must be identified before the thread loosening reaches a certain threshold, very loose states were unnecessary to be considered. Thus the right tapered threads will be adjusted from the 3rd turn to the 4.5th turn with a step increase of 1/4 turn in the experiments to simulate various contact area scenarios and various tightness of the connection.

During the experiment, the Gaussian pulse was generated by a signal processing system, which was shown in Fig. 4. The output was an electrical signal via D/A interface of the NI data acquisition card, and was magnified up to 20 times by the amplifier. At last, the PZT 1 was excited to generate stress waves propagating through the pipeline. The propagating stress wave will be detected by the PZT 2 and transformed into electrical signal, which will be acquired by the computer via A/D interface of the NI data acquisition card. The received signals in various contact scenarios were sampled with a rate of 2 MHz and a duration of 0.1s, which are shown in Fig. 8. The useful signals' strength increased as the contact area increased. However, the background noises were relatively high. It is difficult to calculate the useful signals strength (energy). Table 1 lists the received signal total energies calculated by Eq. (1). Generally speaking, the energy values of received signals increase with the contact area or as the connection tightens. However, it was observed with two exceptions at the cases of 3.5^{th} circle and 4.25^{th} circle. This is maybe caused by background noises.

Using the time reversal technique, the focused signals in corresponding seven contact scenarios were obtained and plotted in Fig. 9. The peak values were much higher than the background noise in all scenarios. The peak amplitude increased along with more contact area. Peak values of these focused signals were listed in Table 2. It is clear that peak values of the focused signals rise monotonously as the contact area increases from 3^{th} circles to 4.5^{th} circles. Trend curves based on energy method and time reversal method were further compared in Fig. 10. From Fig. 10, it can be observed that peak value of the focused signal corresponds to thread tightness correctly. Especially, the peak values at 4.5^{th} circle is just slightly greater than that of 4.25^{th} circle, indicating a trend of saturation, which implies that both scenarios have reached the tightening limit.

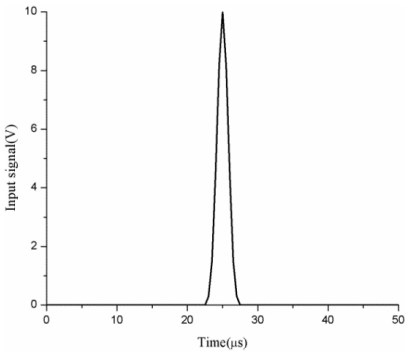

Fig. 7 Pulse signal

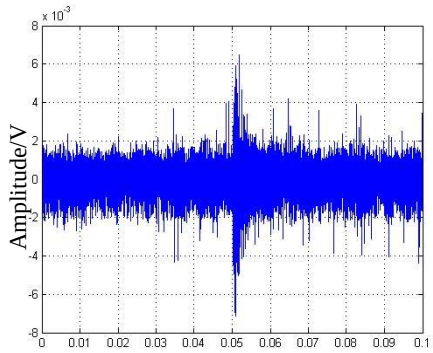

(a)

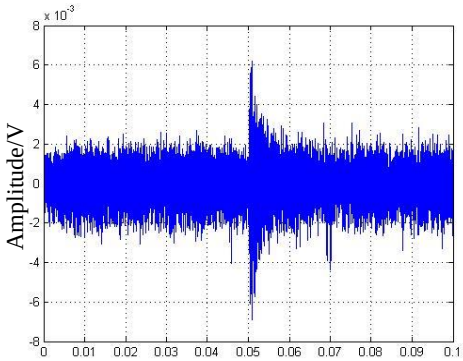

(b)

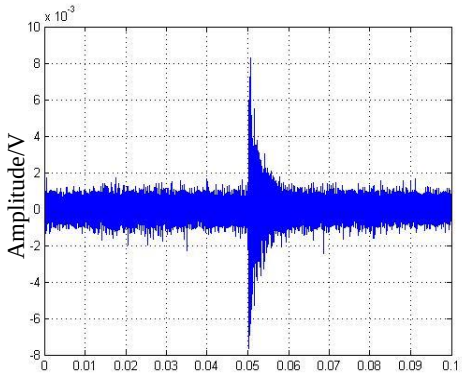

(c)

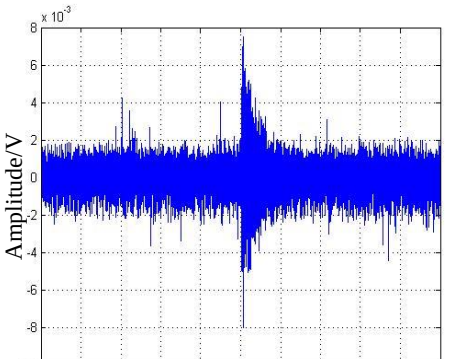

(d)

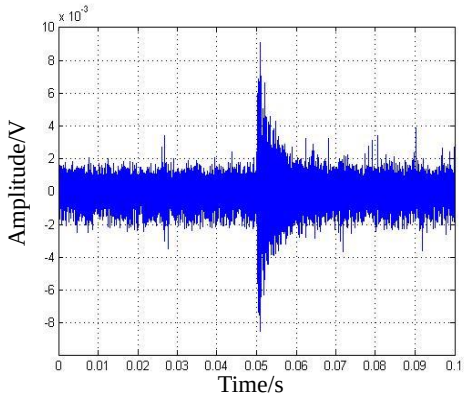

(e)

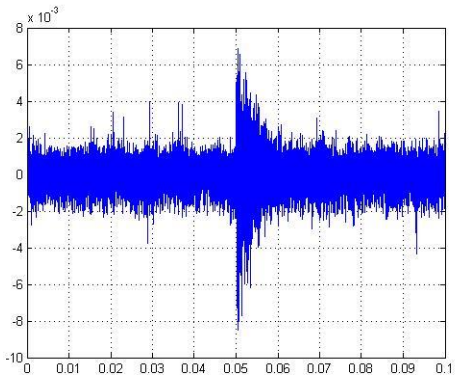

(f)

Continued-

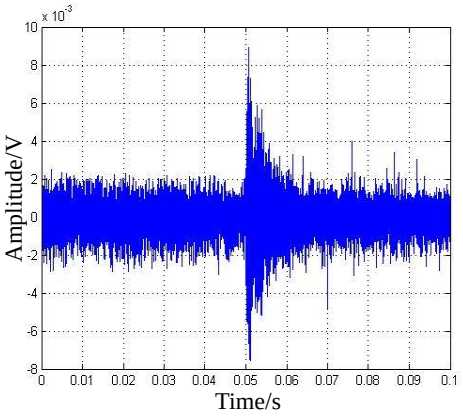

(g)

Fig. 8 Received signals with different contact areas of the right threads (a) Received signal in 3th circle, (b) received signal in 3.25th circle, (c) received signal in 3.5th circle, (d) received signal in 3.75th circle, (e) received signal in 4th circle, (f) received signal in 4.25th circle and (g) received signal in 4.5th circle

Table1. Energy values with different contact areas

Contact area	Energy Value(J)
3th circle	0.0516
3.25th circle	0.0594
3.5th circle	**0.0506**
3.75th circle	0.0672
4th circle	0.0784
4.25th circle	**0.0783**
4.5th circle	0.0828

Using the time reversal technique, the focused signals in corresponding seven contact scenarios were obtained and plotted in Fig. 9. The peak values were much higher than the background noise in all scenarios. The peak amplitude increased along with more contact area. Peak values of these focused signals were listed in Table 2. It is clear that peak values of the focused signals rise monotonously as the contact area increases from 3th circles to 4.5th circles. Trend curves based on energy method and time reversal method were further compared in Fig. 10. From Fig. 10, it can be observed that peak value of the focused signal corresponds to thread tightness correctly. Especially, the peak values at 4.5th circle is just slightly greater than that of 4.25th circle, indicating a trend of saturation, which implies that both scenarios have reached the tightening limit

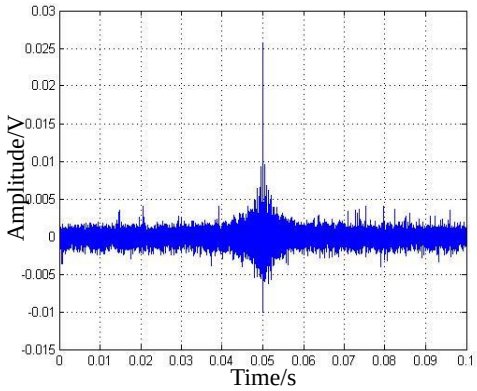

(a)

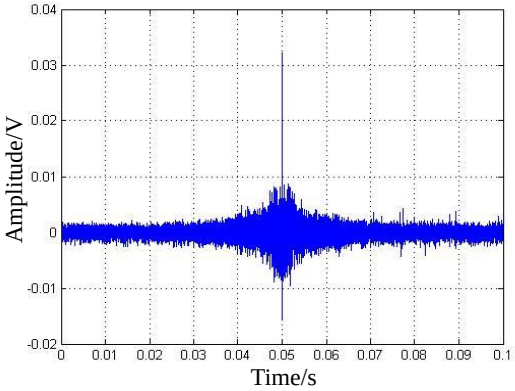

(b)

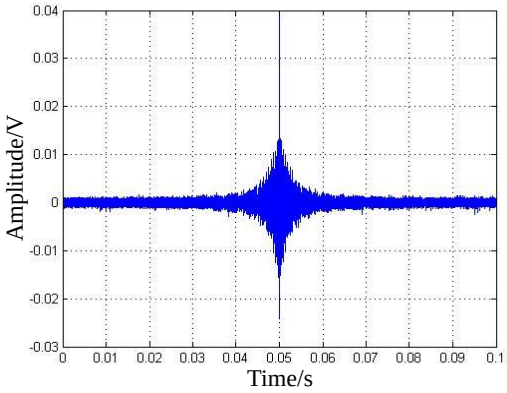

(c)

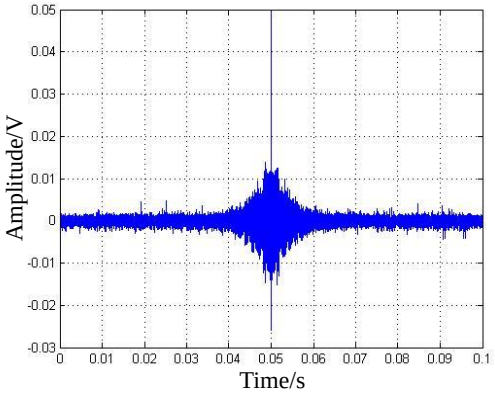

(d)

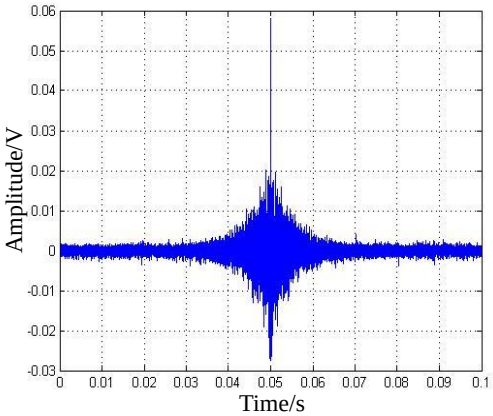

(e)

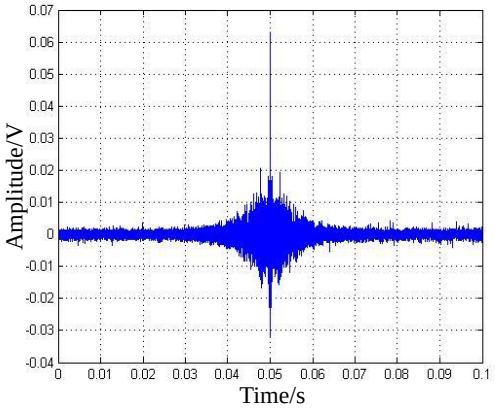

(f)

Continued-

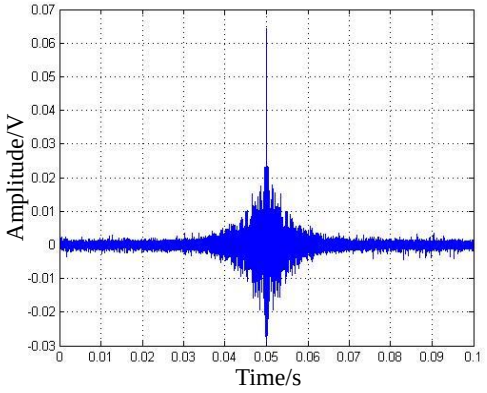

(g)

Fig. 9 Focused signals based on time reversal method with different contact areas (a) Focusing signal in 3th circle, (b) focusing signal in 3.25th circle, (c) focusing signal in 3.5th circle, (d) focusing signal in 3.75th circle, (e) focusing signal in 4th circle, (f) focusing signal in 4.25th circle and (g) focusing signal in 4.5th circle

Table 2 Focused peaks in different contact areas based on time reversal

Contact area	Focused peak value(V)
3^{th} circle	0.0256
3.25^{th} circle	0.0322
3.5^{th} circle	0.0389
3.75^{th} circle	0.0493
4^{th} circle	0.0578
4.25^{th} circle	0.0630
4.5^{th} circle	0.0643

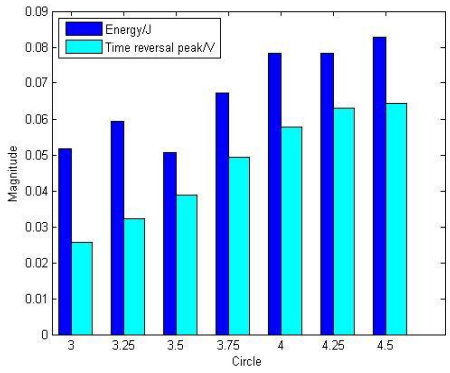

Fig. 10 Trend curve of all different circles for right tapered threads based on energy and time reversal method with fixed 4.25th circle in left threads

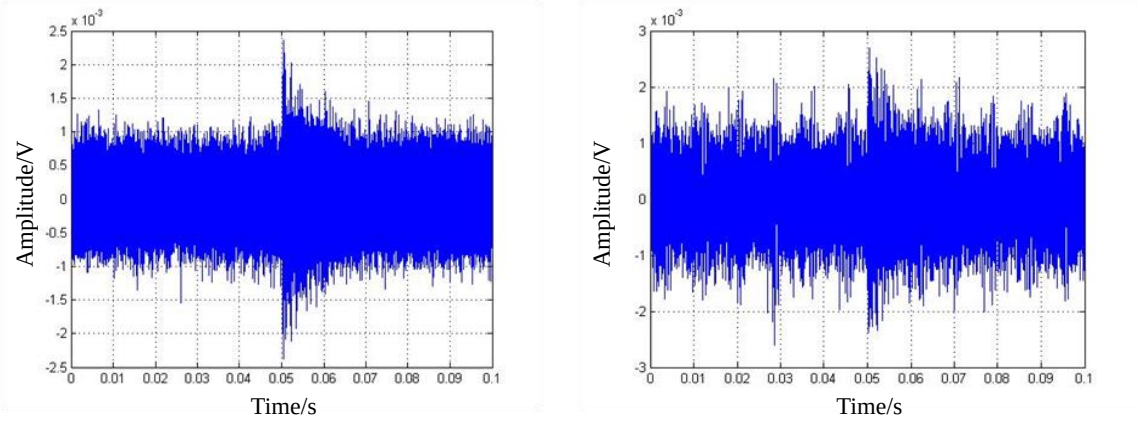

Fig. 11 The received signal at 3th circle in right & 4.25th in left threads with excitation signal amplitude of 2.5 V (a) Received signal without noise background and (b) received signal with noise background

4.2 Anti-noise ability experiments

4.2.1 Anti-noise ability with a different noise background

The experiment in this section aims to demonstrate the anti-noise ability of time reversal method in monitoring thread connection tightness. As described in previous experiments, various contact scenarios, where noises were all completely random, were considered for the test of tapered thread connection tightness, however the focused signal based on time reversal is just able to ignore those noises and focus on the peak value. So one single contact scenario should be enough to clarify the anti-noise ability of the proposed method. Besides, it is much more easily for a loose greatly contact thread to be affected by different noise sources, in which case the anti-noise ability test could be more representative. Therefore, the condition with the left tapered threads as 4.25th circle and the right tapered threads as 3th circle were set in this experiment. The excitation signal amplitude was set to 2.5 V in this experiment. Artificial noise was introduced by rubbing sensor cables when acquiring data. The received signal in the absence of artificial noise is plotted in Fig. 11(a), and the received signals in the presence of artificial noise is shown in Fig. 11(b). Their energies calculated by Eq. (1) were 0.0251J and 0.0478J respectively, which showed the energy value with noise background is almost two times that without noise background. With the time reversal technique, Figs. 12(a) and 12(b) plot the corresponding focused signals, whose peak values were 0.0210 V and 0.0209 V, respectively. The 0.0001 V difference between these two peaks values demonstrated that the focused peak method based on time reversal shows strong anti-noise ability.

4.2.2 Improvement of signal-to-noise ratio (SNR)

The anti-noise ability of the proposed method is verified in section 4.2.1. This section aims to confirm the improved SNR of the proposed method with the time reversal technique. The experiments in this section set the right tapered threads at the 4th circle and the left tapered threads as 4.25th circle. With the same background noise, excitation signal amplitude was increased continually, and the values were 1 V, 2.5 V, 5 V, 7.5 V and 10 V, respectively. Therefore received

signals at different SNR can be obtained. Fig. 13 shows the received signals in the different cases. When the input signal is 1 v, the useful signal was already drown in the noise. With highest amplitude 10 V, the received useful signal was still weak. Their corresponding focused signals using the time reversal technique were shown in Fig. 14, with peak values listed in Table 3. The peak is far larger than the background. The SNR is obviously improved compared to the received signal. The relationship between peak amplitude and input amplitude is shown in Fig. 15. It will be very difficult to obtain the correct index from received signal in a low SNR environment by using energy method, as demonstrated in Fig. 13 a), which shows that the useful signal was totally buried in noise. On the contrary, the time reversal method increases the SNR by focusing a peak amplitude, and the signal can be clearly seen, as demonstrated in Fig. 14 a). From Table 3 and Fig. 15, it is clear that the peak value is proportional as the input amplitude at different SNR level, indicating that the peak value method based on time reversal technique performs with high reliability and repeatability.

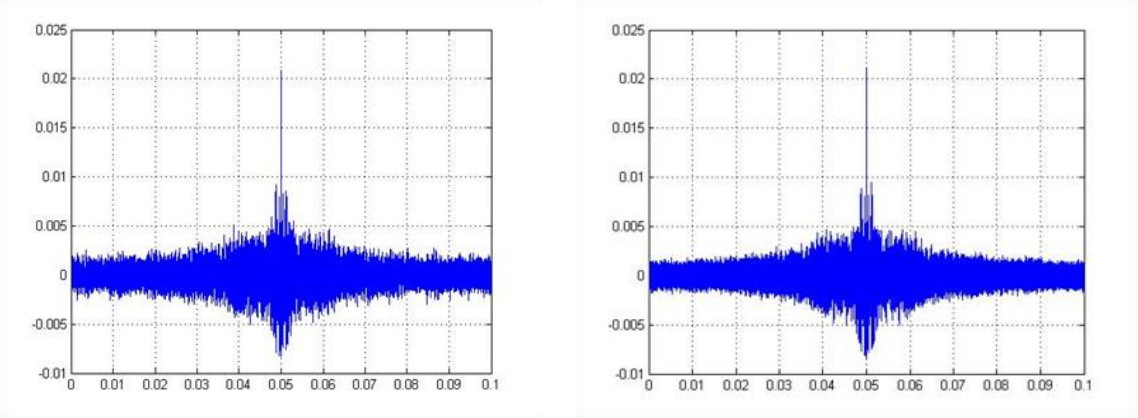

(a) (b)

Fig. 12 The focused signal at 3th circle in right & 4.25th in left threads with excitation signal amplitude of 2.5 V (a) Focused signal without noise background and (b) focusing signal with noise background

Table 3 Focused peaks with different SNR in same contact area

Amplitudes of excitation signal	Time reversal method
1 V	0.0081
2.5 V	0.0201
5 V	0.0438
7.5 V	0.0719
10 V	0.0990

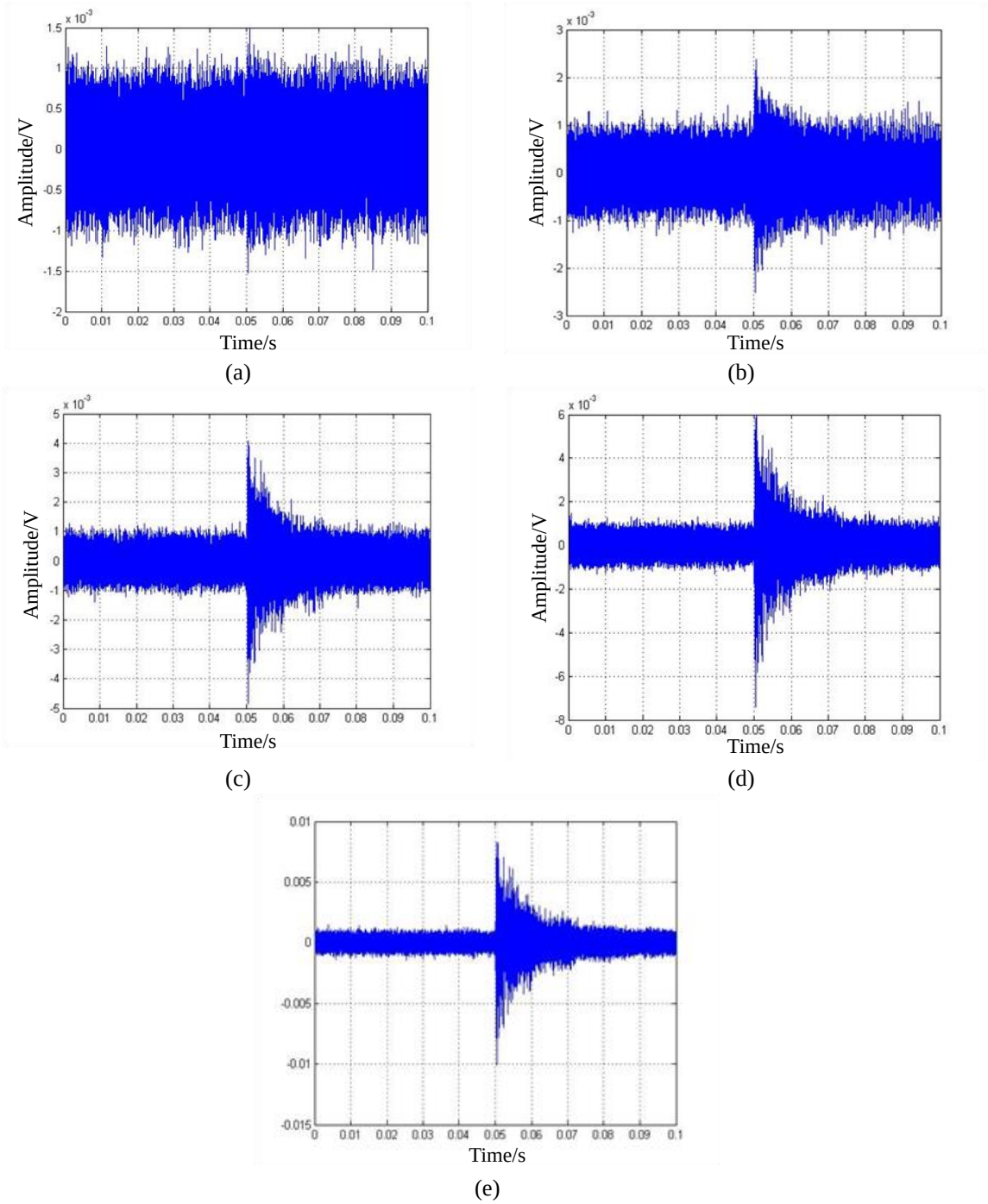

Fig. 13 Received signals at 4th circle in right & 4.25th in left threads with different amplitudes of excitation signal (a) Received signal with excitation signal of 1 V, (b) received signal with excitation signal of 2.5 V, (c) received signal with excitation signal of 5 V, (d) received signal with excitation signal of 7.5 V and (e) received signal with excitation signal of 10 V

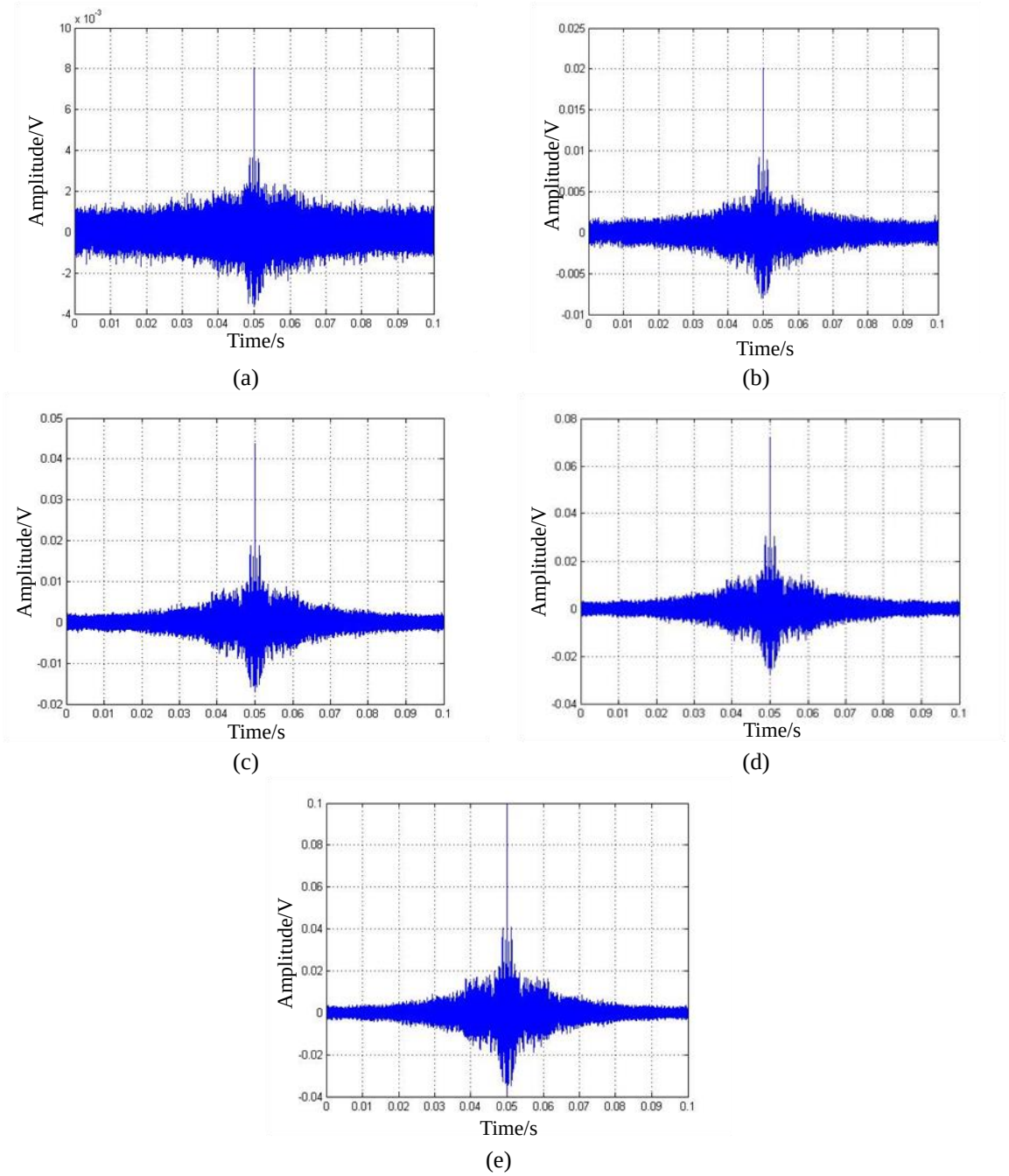

Fig. 14 Focused signals based on time reversal with different amplitudes of excitation signal (a) Focused signal with excitation signal of 1 V, (b) focused signal with excitation signal of 2.5 V, (c) focusesignal with excitation signal of 5 V, (d) focused signal with excitation signal of 7.5 V and (e) focused signal with excitation signal of 10 V

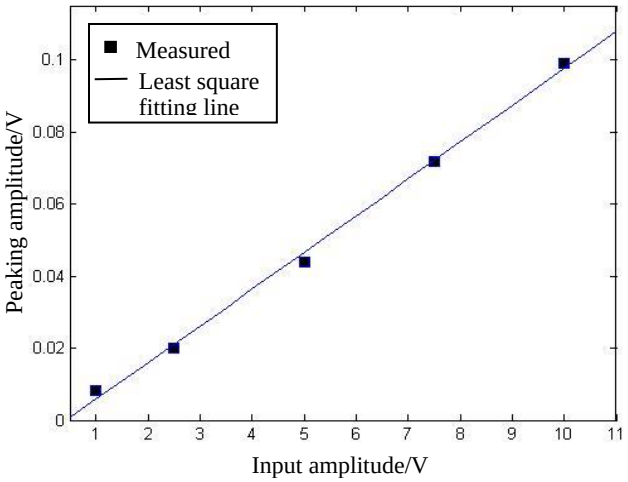

Fig. 15 Relationship between peak amplitude and input amplitude

5. Conclusions

In this paper, an active sensing method using piezoelectric transducers was developed to monitor tapered thread connection for pipeline based on the time reversal technique. From the experimental results of loosening a tapered thread connection, it was found that the focused peaks based on time reversal technique reduced as the tapered threads became looser. Furthermore, the peak value with artificial noise is almost the same as that without noise under the same condition, which indicates that the proposed method possesses the robust anti-noise ability. With the robust anti-noise ability, the proposed method can be reliably used in a low Signal-to-Noise-Ratio (SNR) environment, as demonstrated experimentally. In summary, the experimental results show that the proposed method can monitor the tapered thread connection under different loosening degrees. The proposed active sensing method with piezoelectric transducers has the potential to be implemented in the health monitoring of other large-scale structures with tapered thread connections.

Acknowledgments

The reported research was partially supported by the Major State Basic Research Development Program of China (973 Program, grant number 2015CB057704), the National Science Foundation of China under grant No. 51305141, No. 51121005 (Science Fund for Creative Research Groups), No. 51278084, No. 51478080, Guangdong Province Natural Science Foundation under grant No.2014A030313248 and Guangzhou City Science and Technology Planning Project under grant No. 201509010008 and No.201607010171.

References

Andrieux, S. and Leger, A. (1993), "Multiple scaling method for the calculation of threaded assemblies", *Comput. Method. Appl. M.*, **102**(3), 293-317.

Bouchoucha, F., Akrout, M., Fakhfakh, T., Ichchou, M.N. and Haddar, M. (2012), "Damage detection in cylindrical pipe through diffusion matrix in wave finite element method", *Adv. Struct. Eng.*, **15**(3), 435-445.

Chen, S.J., Zhang, Y., Gao, L.X., Li, Q. and An, Q. (2010), "Loading analysis on the thread teeth in cylindrical pipe thread connection", *J. Press. Vessel T. -ASME*, **132** (3), 1-8.

Ciampa, F. and Meo, M. (2011), "Acoustic emission localization in complex dissipative anisotropic structures using a one-channel reciprocal time reversal method", *J. Acoust. Soc. Am.*, **130**(1), 168-175.

Ciampa, F. and Meo, M. (2012), "Impact detection in anisotropic materials using a time reversal approach", *Struct. Health Monit.*, **11**(1), 43-49.

Damme, B.V., Abeele, K.V.D. and Matar, O.B. (2012), "The vibration dipole: A time reversed acoustics scheme for the experimental localisation of surface breaking cracks", *Appl. Phys. Lett.*, **100**(8), 1-3.

Gangadharan, R., Murthy, C.R., Gopalakrishnan, S. and Bhat, M.R. (2009), "Time reversal technique for health monitoring of metallic structure using Lamb waves", *Ultrasonics*, **49**(8), 696-705.

He, F.J., Cui, X.M., Zhang, Y.H. and Huang, Z.Z. (2003), "Non-contact measurement of oil tube thread and the application", *Proceedings of SPIE* , **5058**, 661-665.

Hong, X.B., Wang, H., Wang, T., Liu, G.X., Li, Y.R. and Song, G.B. (2013), "Dynamic cooperative identification based on Synergetics for pipe structural health monitoring with piezoceramic transducers", *Smart Mater. Struct.*, **22**(3), 1-13.

Jun, Y.J. and Lee, U. (2012), "Computer-aided hybrid time reversal process for structural health monitoring", *J. Mech. Sci. Technol.*, **26**(1), 53-61.

Kokossalakis, G. (2006), "Acoustic data communication system for in-pipe wireless sensor networks" , *Massachusetts Institute of Technology, Phd thesis*, 2006.

Laskar, A., Gu, H.C., Mo, Y.L. and Song, G.B. (2009), "Progressive collapse of a two-story reinforced concrete frame with embedded smart aggregates", *Smart Mater. Struct.*, **18**(7), 1-10.

Li, L.Y., Song, G.B. and Ou, J.P. (2011), "DNN based fault tolerant control of nonlinear structural vibration with actuator faults", *Adv. Struct. Eng.*, **14**(5), 871-879.

Liao, W.I., Wang, J.X., Song, G.B., Gu, H.C., Olmi, C., Mo, Y.L., Chang, K.C. and Loh, C.H. (2011), "Structural health monitoring of concrete columns subjected to seismic excitations using piezoceramic-based sensors", *Smart Mater. Struct.*, **20**(1), 1-10.

Lu, X., Lu, M.Y., Zhou, L.M., Su, Z.Q., Cheng, L., Ye, L. and Meng, G. (2011), " Evaluation of welding damage in welded tubular steel structures using guided waves and a probability-based imaging approach", *Smart Mater. Struct.*, **20**(1), 1-15.

Ma, J., Lowe, M.J.S. and Simonetti, F. (2007), "Measurement of the properties of fluids inside pipes using guided longitudinal waves", *IEEE T. Ultrason. Ferr.*, **54**(3), 647-658.

Ma,J., Lowe, M.J.S. and Simonetti, F. (2007), "Feasibility study of sludge and blockage detection inside pipes using guided torsional waves", *Meas. Sci. Technol.*, **18**(8), 2629-2641.

Mijarez, R., Martinez, F. and Gaydecki, P. (2009), "Continous structural health monitoring guided wave PPM system using steel pipes as communication channel for flood detection in steel offshore oilrigs", *AIP Conf. Proc.*, **1096**,1014-1021.

Parka, H.W., Sohn, H., Lawc, K.H. and Farrard, C.R. (2007), "Time reversal active sensing for health monitoring of a composite plate", *J. Sound Vib.*, **302**(1), 50-66.

Rezaei, D. and Taheri, F. (2010), "Health monitoring of pipeline girth weld using empirical mode decomposition", *Smart Mater. Struct.*, **19**(5), 1-18.

Shahani, A.R. and Sharifi, S.M.H. (2009), "Contact stress analysis and calculation of stress concentration factors at the tool joint of a drill pipe", *Mater. Design*, **30**(9), 3615-3621.

Shi, Z.F. and Zhang, T.T. (2008), "Bending analysis of a piezoelectric curved actuator with a generally

graded property for Piezoelectric parameter", *Smart Mater. Struct.*, **17**(4), 1-7.
Song, G., Gu, H.C. and Mo, Y.L. (2008), "Smart aggregates: multi-functional sensors for concrete structures - a tutorial and a review", *Smart Mater. Struct.*, **17**(3), 1-17.
Song, G., Gu, H.C., Mo, Y.L., Hsu T.T.C. and Dhonde, H. (2007), "Concrete structural health monitoring using embedded piezoceramic transducers", *Smart Mater. Struct.*, **16**(4), 959-968.
Song, G., Mo, Y.L., Otero, K. and Gu, H.C. (2006), "Health monitoring and rehabilitation of a concrete structure using intelligent materials", *Smart Mater. Struct.*, **15**(2), 309-314.
Tua, P.S., Quek S.T. and Wang, Q. (2005), "Detection of cracks in cylindrical pipes and plates using piezo-actuated lamb", *Smart Mater. Struct.*, **14**(6), 1325-1342.
Vigoureux, D. and Guyader, J.L. (2012), "A simplified time reversal method used to localize vibrations sources in a complex structure", *Appl. Acoust.*, **73**(5), 491-496.
Wang, T., Song, G., Wang, Z.G. and Li, Y.R. (2013), "Proof-of-concept study of monitoring bolt connection status using a piezoelectric based active sensing method" , *Smart Mater. Struct.*, **22**(8), 1-5.
Wang, X.J., Tse,P.W., Mechefske, C.K. and Hua, M. (2010), " Experimental investigation of reflection in guided wave-based inspection for the characterization of pipeline defects" , *NDT& E Int.*, **43**(4), 365-374.
Watkins, R. and Jha, R. (2012), "A modified time reversal method for Lamb wave based diagnostics of composite structures", *Mech. Syst. Signal Pr.*, **31**(8), 345-354.
Yang, J. and Chang, F.K. (2006), " Detection of bolt loosening in C–C composite thermal protection panels: I. Diagnostic principle", *Smart Mater. Struct.*, **15**, 581-590.

BS